

The Effect of pH on Coupled Mass Transfer and Sol–Gel Reaction in a Two-Phase System

H. J. Castelijns,^{†‡} H. P. Huinink,[‡] L. Pel,[‡] and P. L. J. Zitha^{*,†}

Department of Civil Engineering and Geosciences, Delft University of Technology, P.O. Box 5048, 2600 GA Delft, The Netherlands, and Department of Applied Physics, Eindhoven University of Technology, P.O. Box 513, 5600 MB Eindhoven, The Netherlands

Received: April 26, 2007; In Final Form: August 5, 2007

The coupled mass transfer and chemical reactions of a gel-forming compound in a two-phase system were recently analyzed in detail [Castelijns et al. *J. Appl. Phys.* **2006**, *100*, 024916]. In this successive work, the gel-forming chemical tetramethylorthosilicate (TMOS) was dissolved in a mineral oil and placed together with heavy water (D₂O) in small cylinders. The transfer of TMOS from the oleic phase to the aqueous phase was monitored through nuclear magnetic resonance (NMR) relaxation time measurements of hydrogen in the oleic phase. The rate of gelation was measured through NMR relaxation time measurements of deuterium in the aqueous phase. The temperature, the initial concentration of TMOS, and the type of buffer in the aqueous phase were varied in the experiments. The mass transfer is driven by the rate of hydrolysis, which increases with temperature. The hydrolysis rate is the lowest at a neutral pH and is the highest at a low pH. In the aqueous phase, a sharp decrease in the transverse relaxation time (*T*₂) of ²H is observed, which is attributed to the gel reaction. The plateau in *T*₂ indicates the gel transition point. The gel rates increase with increasing temperature and increasing concentration, and are the highest at a neutral pH.

1. Introduction

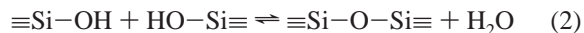
Silica gels can be produced by the hydrolysis of an alkoxy-silane precursor in an aqueous solution. The product of the hydrolysis reaction, that is, silanol (Si–OH) groups, condenses into silica aggregates, ultimately leading to gelation of the solution. Instead of mixing the alkoxy-silane directly with water, which requires a homogenization agent such as alcohol,¹ the precursor may be introduced into water gradually through a separate oleic phase in contact with the water. In that case, the alkoxy-silane is initially present in the oleic phase. Upon contact with the aqueous phase, the alkoxy-silane partitions between both phases and forms a gel in the aqueous phase.

An application of this process was first proposed by Plazanet and Thomere for the consolidation of sand producing formations during oil recovery.² Second, the process could be applied as a means to reduce water production during oil recovery.³

In the aqueous phase, the chemical hydrolyzes into silanol and its conjugate alcohol. The process is illustrated in Figure 1 for a two-phase bulk system. In the case of full hydrolysis, the reaction is according to



Both reaction products remain in the aqueous phase. The formation of the alcohol increases the solubility of the precursor in water. This effect, together with the depletion of the alkoxy-silane, leads to a full transfer of the compound from the oleic to the aqueous phase.^{4,5} As the silanol is formed, the following condensation reaction concurrently occurs:



The rate of both reactions is sensitive to temperature, concentration, and pH.^{1,6} The reactions described by eqs 1 and 2 represent a simplification of the complicated reaction pathways; that is, the condensation and particle formation may also occur between partly hydrolyzed (intermediate) reaction products. However, in the context of the coupled mass transfer and sol–gel reaction in the two-phase system, the equations are adequate to describe the reactive part of the process.

Recently, the mechanisms of the coupled mass transfer and gelation process of tetramethylorthosilicate (TMOS) were analyzed in two-phase bulk systems using dedicated nuclear magnetic resonance (NMR) techniques.^{4,5} TMOS was dissolved in *n*-hexadecane and placed together with demineralized water (H₂O) in small cylinders. The concentration of TMOS and the temperature were varied, and their effect on the mass transfer rate and gelation time was determined.

The aim of this work is to further analyze the effect of temperature, concentration, and type of buffer on the reaction and mass transfer rates. Since the solubility of TMOS in water plays an important role for the partitioning behavior, the formation of methanol due to hydrolysis is expected to affect the mass transfer process. TMOS was dissolved in a mineral oil and placed in small cylinders together with heavy water (D₂O) with or without buffer. A simple model, which was previously developed,⁵ is used to extract the hydrolysis rates. The purpose of using heavy water, compared to using normal water, is to enable a straightforward interpretation of the NMR relaxation time measurements of the aqueous phase

2. Theoretical Background

2.1. Mass Transfer and Hydrolysis. Consider a volume comprising two liquid phases (see Figure 1). The lower phase initially consists of heavy water, and the upper phase consists

* Author to whom correspondence should be addressed. E-mail: p.l.j.zitha@tudelft.nl, tel.: +31 15 2788437, fax.: +31 15 2781189.

[†] Delft University of Technology.

[‡] Eindhoven University of Technology.

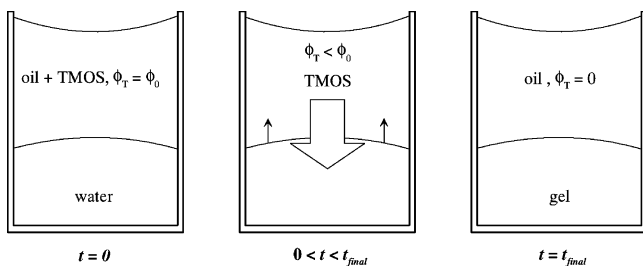


Figure 1. Cylindrical (hydrophobic) container with two liquid phases separated by an interface. The upper phase initially consists of TMOS dissolved in oil with a concentration of $\phi_T = \phi_0$. The lower phase is water. From the instant the phases are brought together, the TMOS partitions into the aqueous phase. Because of the hydrolysis of TMOS in water, the TMOS transfers completely to the aqueous phase in the course of time. At $t = t_{\text{final}}$, the concentration ϕ_T is zero, and the water has turned into a gel.

of a solution of TMOS in oil with an initial volume concentration $n_i(0)$, which corresponds to a volume fraction ϕ_0 . From the moment the phases are put together, the TMOS partitions into the aqueous phase where it undergoes the heterogeneous reaction. The system is relatively small (on the order of centimeters). The overall mass transfer is governed by the chemical reaction rate in the aqueous phase. Each phase is well-mixed (based on observations in previous experiments⁴), so that diffusion or convection processes do not limit the mass transfer. Theoretically, the depletion of TMOS in the oleic phase at the interface and the downward flux of TMOS in the aqueous phase give rise to density gradients. However, the density gradients are diminished by convection due to the effect of gravity. The mass transfer is therefore assumed to be fast compared to the chemical reactions.

A conceptual model was proposed⁵ to describe the overall flux of TMOS between the phases.

The change in the total number of TMOS molecules n_t in the system as a function of time is described by the following kinetic equation:

$$\frac{dn_t}{dt} = \frac{d(n_o + n_w)}{dt} = -kn_w \quad (3)$$

where n_o and n_w are the number of TMOS molecules in the oleic and aqueous phases, respectively, and k is the rate of hydrolysis (where we assume full hydrolysis of the TMOS molecules). The ratio between n_o and n_w at each instant is determined by the solubility of TMOS in both phases through the following partitioning equation:

$$\frac{n_w}{n_w + m_w} = \frac{n_o}{n_o + m_o} \exp\left(-\frac{\epsilon(n_m)}{RT}\right) \quad (4)$$

where m_w is the total number of water, methanol, and silicic acid molecules, m_o is the number of hydrocarbon molecules, R is the gas constant, T is the temperature, and ϵ is an interaction parameter that depends on the methanol concentration n_m . The exact choice of $\epsilon(n_m)$ is arbitrary, but the parameter should decrease with an increasing value of n_m and vice versa. As a first-order approximation, the parameter ϵ is chosen as

$$\epsilon = \epsilon_0 \left[1 - \alpha \frac{n_m}{m_w(0)} \right] \quad (5)$$

where ϵ_0 is the interaction parameter in the absence of methanol, and α is an arbitrary scale factor. The methanol concentration n_m increases in the course of time as given by

$$n_m = 4 \int_0^t kn_w(\tau) d\tau = 4[n_i(0) - n_i(t)] \quad (6)$$

The variables n_w and m_w in eq 4 are rewritten in terms of n_o and m_o . Then, by rearranging eq 3, the following differential equation is obtained:

$$\frac{dn_o}{dt} = -kEn_o[N - (n_o + m_o)] \times \frac{\{(n_o + m_o) + 4\epsilon_0\alpha\beta En_o[N - (n_o + m_o)]\}}{Enm_o + (1 - E)(n_o + m_o)^2} \quad (7)$$

where $E = \exp(-\epsilon/RT)$, $\beta = (RT)^{-1}$, and N is the total number of particles, which is constant. Equation 7 can be solved numerically and optimized to fit the experimental data, yielding the parameters ϵ_0 and k . The parameter α is not optimized to limit the number of parameters in the optimization. We choose $\alpha = 1$, so that E (and thus the solubility of TMOS in water) increases significantly during the reactive transport, depending on ϵ_0 and given the estimated final amount of methanol (see Figure 2 for an example calculation of E).

2.2. NMR Relaxation of Deuterium in Sol–Gel. For a rigorous introduction to nuclear magnetic relaxation, we refer to the work of Abragam.⁷ In the gelling solution, the deuterium nuclei are most abundant in the form of D_2O molecules. The main relaxation mechanism for deuterium nuclei (deuterons) in D_2O is due to quadrupolar interaction between the deuterons and the internal electric field gradient at the nuclei. This intramolecular relaxation is driven by molecular fluctuations, such as molecular rotation. The fluctuations are often characterized by a molecular correlation time τ_c .⁷

In the gelling solution, the water molecules diffuse through the system, and, with a certain probability, they adsorb onto or interact with the silica clusters. The molecules near a silica surface or adsorbed on the surface may exhibit anisotropic motion⁸ or even exhibit “ice-like” behavior.⁹

One can assign different phases in which a molecule or nucleus resides during a certain life time.^{8,10} Each phase i has a transverse relaxation time $T_{2,i}$ brought about by an effective correlation time $\tau_{c,i}$. The shorter $\tau_{c,i}$, the longer is $T_{2,i}$.⁷ The silica is dispersed on the scale of nanometers. Because of diffusion, the water molecules distant from the silica surface will exchange relatively quickly with the water molecules at the surface. A straightforward, simple method is to assign a bulk relaxation time $T_{2,b}$ to the molecules distant from the surface and a relaxation time $T_{2,s}$ to the molecules at the surface, say within a monolayer adsorbed to the surface.¹¹ The average relaxation time in this two-phase model is given by¹⁰

$$T_{2,AV}^{-1} = \frac{f_s}{T_{2,s}} + \frac{1 - f_s}{T_{2,b}} \quad (8)$$

In general $T_{2,s} < T_{2,b}$ and $f_s < 1$. The fraction f_s is proportional to the specific surface area A (per unit volume) of the silica surface. Further, suppose the interaction between the solid and liquid is limited to a single monolayer of liquid molecules, then the fraction f_s is approximated by

$$f_s = \frac{A\lambda}{1 - \phi_m} \quad (9)$$

where λ is the thickness of the monolayer, and ϕ_m is the volume fraction of the solid silica content in the gel.

Because of the hydrolysis reaction, methanol is formed, which is mixed with the water. It is known that, in mixtures of

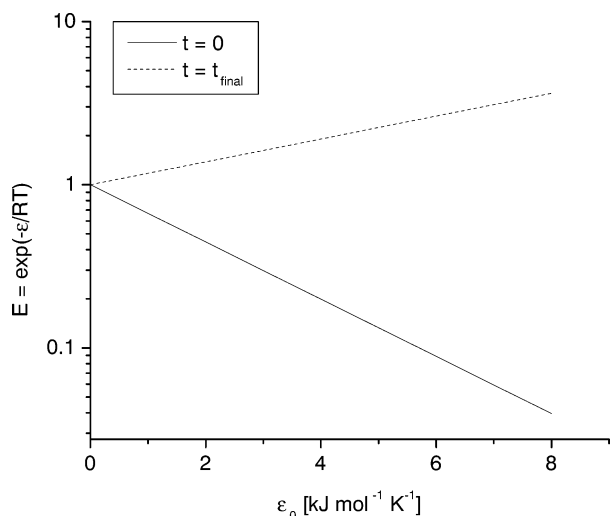


Figure 2. Partitioning coefficient E as a function of the interaction coefficient ϵ_0 for $t = 0$ and $t = t_{\text{final}}$ (which represent complete mass transfer and hydrolysis). The calculations, using eq 5 with $\alpha = 1$, are based on a temperature of 25 °C and an initial volume fraction $\phi_T = 0.35$.

methanol and water, the molecular reorientation time of the water molecules is a function of the methanol concentration. Depending on the temperature, the reorientation time can increase up to 100% with increasing methanol concentration.^{12,13} Therefore, $T_{2,b}$ is a function of the methanol concentration n_m in the gelling solution:

$$T_{2,b} = g(n_m, T) \quad (10)$$

where g is an empirical function that can be determined by calibration.

3. Experiment

3.1. Materials. TMOS (> 99% pure) was dissolved in Isopar V, a mineral oil (from ExxonMobil) with a viscosity of about 10 mPa s at room temperature. For the aqueous phase, we used D₂O (99.9% pure). Methanol (99% pure) was mixed with heavy water for calibration measurements of T_2 . Untreated D₂O was used for the calibration mixtures. For the bulk experiments, three different buffers were prepared to control the pH by adding salts and chemicals containing normal hydrogen. The pH was measured with a semiconductor-type pH meter. The low pH buffer (pH = 2.95) contained 8.47 g of citric acid, 3.22 g of NaOH, and 2.18 g of HCl per liter; the intermediate pH buffer (pH = 5.50) contained 12.53 g of citric acid and 6.32 g of NaOH per liter; and the high pH buffer (pH = 9.48) contained 3.81 g of disodiumtetraborat per liter. Pure D₂O was used as well in the experiments. Calibration gel samples were prepared by mixing TMOS with each buffer in various volume fractions ϕ_T^g . The gel samples were aged at room temperature for 20 days. All gelling solutions turned into a macroscopic gel; that is, the cross-linking gel particles percolated the entire volume of the samples, except for the gelling solution prepared with a TMOS concentration of $\phi_T^g = 0.10$ in the pH = 9.48 buffer, even after 20 days of aging. All gels were transparent, but the gels prepared with the pH = 5.50 buffer were partly turbid. The two-phase bulk experiments were performed using cylindrical Teflon vials with an inner diameter of 18 mm. In each experiment, 2.5 mL of water and 2.5 mL of TMOS/oil were placed in the vial. The initial volume fraction of TMOS, $\phi_T(0)$, was 0.20 or 0.35.

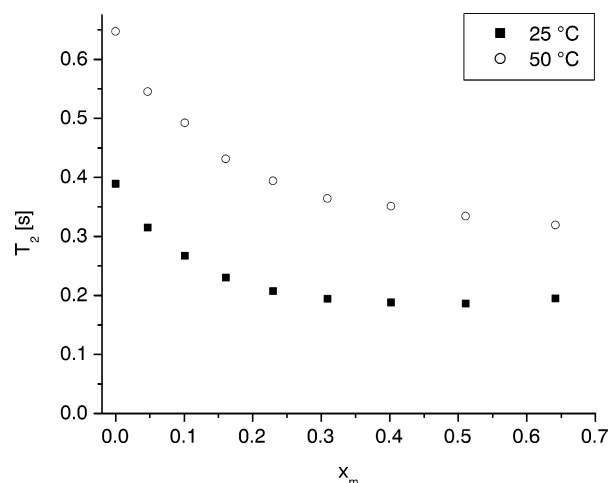


Figure 3. T_2 of the ^2H content in the methanol–D₂O calibration mixtures. x_m is the mole fraction of methanol. The temperature is indicated in the legend.

3.2. NMR Measurements. Relaxation times for ^1H and ^2H in the samples were measured with a 0.95 T NMR scanner (home-built) operating at a frequency of 40.5 MHz for hydrogen and 6.21 MHz for deuterium. The setup consists of an electromagnet with a vertical, narrow-bore insert with an inner diameter of 31 mm. The insert is capable of producing a static magnetic gradient up to 0.2 T/m in the vertical direction. A single radio frequency (rf) coil is used with two different front-end rf circuits for ^1H and ^2H , respectively. Switching between the two circuits takes less than a second, allowing for a fast sequential NMR measurement of hydrogen and deuterium. A poly(vinyl chloride) sample holder was constructed in which a fluorocarbon fluid (Galden HT135, manufactured by Solvay Solexis) was circulated in order to control the temperature of the sample. The fluid is invisible to the NMR setup, and the temperature can be controlled between 10 and 55 °C with an accuracy of about 1°.

Details about the sequences can be found in a previous work.⁴ To summarize, the T_1 of the hydrogen content in the oleic phase is measured to determine the TMOS concentration in oil, and the T_2 of the aqueous phase is measured to monitor the progress of gelation. In this case, T_2 is measured for the deuterium content. Here, a one-dimensional static magnetic gradient is used. Since in previous measurements⁴ the phases showed no significant spatial profiles in T_1 or T_2 , it was decided to measure a single slice in the oleic phase and a single slice in the aqueous phase, in order to limit the total acquisition time. The measurements were repeated for each sample over an interval of 20–40 h.

4. Results and Discussion

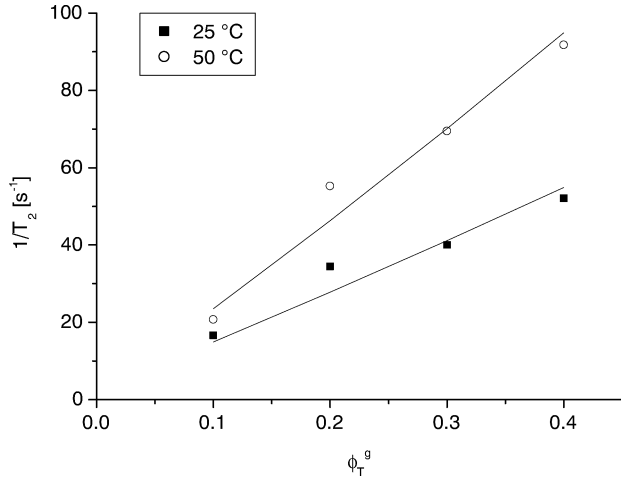
4.1. Calibration Experiments. **4.1.1. Methanol–D₂O Calibrations.** The results of the relaxation time measurements are shown in Figure 3. At 25 °C, the T_2 for D₂O is 0.389 s and decreases with an increasing molar ratio of methanol, x_M , to 0.186 s when $x_M = 0.511$. At 50 °C, the T_2 for D₂O is 0.647 s and decreases with an increasing molar ratio of methanol, x_M , to 0.319 s when $x_M = 0.642$. The effect of mixing methanol with D₂O on the observed T_2 of the water molecules appears to be less pronounced than in the case of H₂O,⁴ but agrees well with other studies on methanol–water mixtures.^{12,13}

4.1.2. Calibration Gel Samples. The transverse relaxation time T_2 of deuterium was measured in the gels at 25 and 50 °C, respectively. The results are listed in Table 1. In all cases, the

TABLE 1: Transverse Relaxation Time T_2 of Deuterium in Aqueous Buffers and of Deuterium in Calibration Gel Samples

ϕ_T^g	T_2 [s]							
	no buffer		pH = 2.95		pH = 5.50		pH = 9.48	
	25 °C	50 °C	25 °C	50 °C	25 °C	50 °C	25 °C	50 °C
0.00	0.389	0.647		0.652		0.642		0.652
0.10	0.123	0.073	0.060	0.048	0.028	0.025	0.047	0.077
0.20	0.066	0.037	0.029	0.018	0.021	0.018	0.013	0.017
0.30	0.053	0.030	0.025	0.014	0.018	0.015	0.0084	0.0081
0.40	0.038	0.026	0.019	0.011	0.016	0.013	0.0077	0.0057

^a ϕ_T^g is the initial volume fraction of TMOS mixed with water to prepare the gels.

**Figure 4.** Reciprocal transverse relaxation time, $1/T_2$, of deuterium in the acid-catalyzed gels (pH = 2.95). The solid curves indicate the obtained fits using eq 8 and the approximation for f_s .

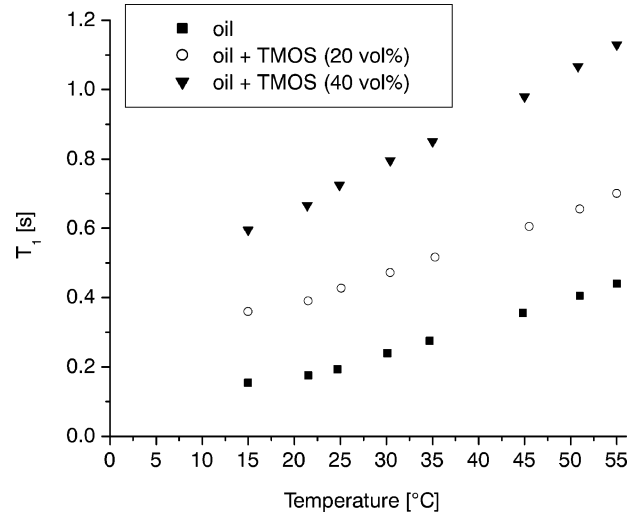
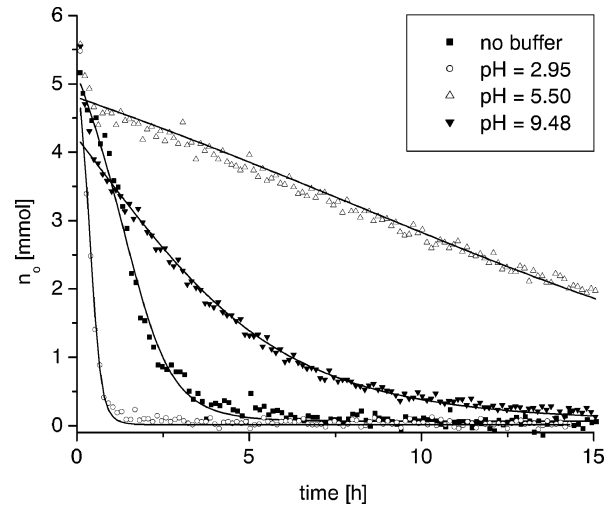
relaxation time T_2 decreases with increasing initial TMOS concentration ϕ_T^g . The reciprocal relaxation times are shown for the pH = 2.95 gels in Figure 4. The relaxation times for deuterium in the gels were fitted with eq 8 using eq 9 to estimate f_s . Furthermore, the approximation $\phi_m = 0.2 \phi_T^g$ was used, which is based on full hydrolysis and condensation of the initial TMOS content. Typical experimental values of the surface area of aerogels, with which the dilute wet gels are compared, are on the order of $1000 \text{ m}^2 \text{ g}^{-1}$,¹⁴ so we choose $A = 1000 \text{ m}^2 \text{ g}^{-1}$ for the calculation of f_s . The monolayer thickness λ equals 1.5 \AA . The bulk relaxation time $T_{2,b}$ of the water–methanol mixture in the pores, which is a function of ϕ_T^g , is derived from the calibration results of the water–methanol mixtures together with the calculation of the final water–methanol ratio in the gels. The resulting fits for the acid-catalyzed gels are shown in Figure 4. It can be observed that the reciprocal relaxation times increase roughly linearly with ϕ_T^g . The obtained surface relaxation times $T_{2,s}$ are listed in Table 2. The transverse relaxation times $T_{2,s}$ are on the order of $0.1\text{--}1 \text{ ms}$. The calculated fraction f_s varied between 0.0067 and 0.028 .

4.2. Two-Phase Bulk Experiments. **4.2.1. Concentration Graphs.** The average TMOS concentration in the oleic phase in the two-phase bulk experiments was determined by measuring T_1 of the oleic phase.⁴ For this purpose, calibrations of T_1 for TMOS/Isopar V mixtures were made (see Figure 5), which clearly showed a monotonous increase of T_1 with increasing TMOS concentration and temperature within the temperature range considered ($15\text{--}55 \text{ }^\circ\text{C}$). From the derived volume fraction of TMOS in oil, the number of TMOS molecules n_o in the oleic phase was calculated. The results of four bulk experiments, done

TABLE 2: Results of the Least-Square Fit on the Relaxation Time Data (for Deuterium) of the Calibration Gels Using Eq 8 and the Approximation for f_s

pH	T [°C]	$T_{2,s}^a$ [ms]
no buffer	25	1.33 ± 0.04
	50	0.70 ± 0.06
2.95	25	0.57 ± 0.04
	50	0.31 ± 0.01
5.50	25	0.41 ± 0.06
	50	0.33 ± 0.04
9.48	25	0.21 ± 0.02
	50	0.18 ± 0.02

^a The surface relaxation terms, $T_{2,s}$, are given for each series at both temperatures.

**Figure 5.** Average relaxation time T_1 of hydrogen in TMOS/Isopar V (oil) mixtures as a function of temperature. The concentration of TMOS is indicated in the legend.**Figure 6.** Concentration of TMOS in the oleic phase as a function of time. The temperature was controlled to $25 \text{ }^\circ\text{C}$. The type of buffer used is indicated in the legend. The solid curves are the fitted concentration profiles using the optimization described in Section 2.

at $25 \text{ }^\circ\text{C}$ with varying pH of the aqueous phase and with an initial volume fraction $\phi_T(0)$ equal to 0.35 , are shown in Figure 6. For the pH = 9.48 case, initially, the number of molecules n_o is close to the initial number ($n_o(0) = 5.88 \text{ mmol}$), after which it drops gradually to almost zero within 15 h . The unbuffered system shows a similar but faster decay, and the concentration is almost zero within 5 h . The lower pH system (pH = 2.95) shows the fastest decay, and the mass transfer is complete within

TABLE 3: Fitted Hydrolysis Rate k and Interaction Parameter ϵ_0 for the Various Bulk Experiments

pH	T [°C]	$\phi_T(0)$	k [10^{-3} s^{-1}]	ϵ_0 [kJ mol $^{-1}$]	gel time ^a [h]
no buffer	25	0.20	0.246 ± 0.008	2.8 ± 0.1	8 ± 1
		0.35	0.323 ± 0.009	4.6 ± 0.1	6 ± 1
	50	0.20	0.43 ± 0.02	4.6 ± 0.2	2.0 ± 0.5
		0.35	0.51 ± 0.03	4.9 ± 0.02	1.0 ± 0.5
2.95	25	0.20	0.32 ± 0.01	0.9 ± 0.1	30 ± 3
		0.35	1.39 ± 0.06	5.1 ± 0.2	14 ± 2
	50	0.20	1.05 ± 0.05	2.9 ± 0.2	5 ± 1
		0.35	2.4 ± 0.3	6.1 ± 0.6	2.5 ± 0.5
5.50	25	0.20	0.049 ± 0.001	1.95 ± 0.04	2.0 ± 0.5
		0.35	0.032 ± 0.001	3.79 ± 0.02	1.5 ± 0.5
	50	0.20	0.127 ± 0.003	5.45 ± 0.08	1.0 ± 0.5
		0.35	0.094 ± 0.002	5.29 ± 0.08	<0.5
9.48	25	0.20	0.090 ± 0.002	1.91 ± 0.08	no percolation
		0.35	0.088 ± 0.001	2.63 ± 0.04	6 ± 1
	50	0.20	0.54 ± 0.03	3.6 ± 0.2	no percolation
		0.35	1.18 ± 0.07	5.5 ± 0.2	1.0 ± 0.5

^a The gel time is derived from the point at which T_2 of ^2H reaches a minimum or plateau.

2 h. The lowest mass transfer rate was observed in the intermediate pH system (pH = 5.50). The mass transfer is complete after 40 h. Test experiments in transparent vials revealed that a weak and turbid gel was formed quickly within 2 h in the intermediate pH systems, despite the limited transfer of TMOS within the initial 2 h. Still, the TMOS transfers completely to the aqueous phase, and the gel does not appear to form an impermeable barrier.

The concentration graphs of all bulk experiments were fitted by optimizing the solution of eq 7, modified to include an additional offset and show a good fit, except at small times. Because of the instant partitioning in the model, the fit curves tend to start below the real initial concentration. From the fits, the hydrolysis rate k and the interaction parameter ϵ_0 were derived, all of which are listed in Table 3. Ideally, the derived hydrolysis rate k and interaction parameter ϵ_0 should be independent of the initial concentration of TMOS used in the experiment. For most of the experiments, the values agree within a factor of 2 with respect to $\phi_T(0) = 0.20$ and 0.35 , respectively. The results for the pH = 2.95 system show a bigger discrepancy. Nevertheless, considering the simplicity of the model, the results are satisfactory and qualitatively reveal the effect of pH on the hydrolysis rate, which in turn drives the mass transfer. The hydrolysis rate k is on the order of 10^{-5} to 10^{-3} s^{-1} . Increasing the temperature always resulted in an increased value for k , which is expected. The magnitude of the increase, however, varies among the systems, that is, the factor is between 1.6 and 13. The strongest dependence of k on temperature is found in the high pH system. The lowest values for k are found when the pH is equal to 5.50, which is close to neutral conditions. Both the lower and higher pH systems show a higher hydrolysis rate, which agrees well with the literature.^{1,6} Hydrolysis is promoted under acid-catalyzed conditions as the alkoxide groups are more easily protonated and attacked by water. Under base-catalyzed conditions, the abundant hydroxyl anions attack the silicon atoms.¹

4.2.2. T_2 of the Aqueous Phase. For the same systems, the transverse relaxation time T_2 of the ^2H content in the aqueous phase was measured. The results are shown in Figure 7 for $T = 25^\circ\text{C}$ and $\phi_T(0) = 0.35$. The T_2 versus time graphs are smooth and exhibit almost no scatter. In the systems at $T = 25^\circ\text{C}$, T_2 is initially about 350 ms (similar to the bulk value of D_2O) and decreases gradually to values below 100 ms within several hours. However, the graphs show a significant difference. In the pH = 9.48 system, the T_2 decreases relatively quickly to

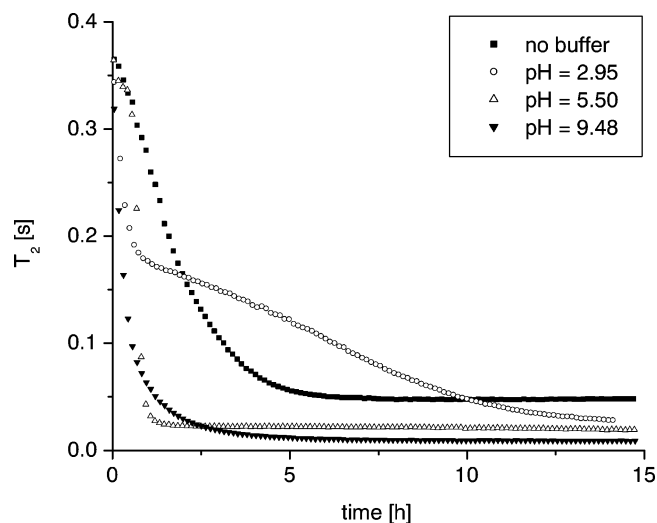


Figure 7. T_2 of the ^2H content in the aqueous phase as a function of time. The measurements were done at 25°C using four different D_2O solutions. The initial concentration $\phi_T(0)$ was 0.35.

100 ms within the first 5 h, after which it decreases slowly and monotonically to 30 ms during the remainder of the experiment (up to $t = 47$ h). A stabilization of T_2 or plateau is observed after 6 h. In the pH = 2.95 system, the T_2 decreases quickly from 335 to 250 ms in the first hour, after which it decreases more slowly to 34 ms in the remainder of the experiment (up to $t = 47$ h). The T_2 in the unbuffered system starts at 360 ms and decays to 73 ms in the first 10 h of the experiment. In the pH = 5.50 system, the T_2 decreases most rapidly and reaches a plateau at $T_2 = 21$ ms after 1.5 h. The decay of T_2 is due to the cross-linking of the silica, which indicates that the condensation rate is low for the pH = 2.95 system compared to the other systems. The condensation rate appears to be the highest for the pH = 5.50 system, which corresponds to the fast gel formation observed in the transparent vials. Test measurements with the transparent vials also revealed that the gel formed in the pH = 9.48 system with $\phi_T(0) = 0.20$ did not percolate in the entire volume of the aqueous phase and remained liquid-like. Despite complete transfer of TMOS and the fast condensation in the higher pH system, the lack of percolation suggests that the silicic acid initially condenses into larger aggregates compared to the lower pH systems, which is expected.¹ As a result, the formed clusters consist of colloidal particles rather than a highly branched network.

In the systems at $T = 50^\circ\text{C}$, T_2 is initially about 630 ms in the unbuffered system and drops to 58 ms within 2 h. The T_2 in the buffered systems is initially shorter, around 540 ms, which is due to the already significant degree of hydrolysis in the initial minutes of the experiment. In the lower pH system, T_2 drops to 20 ms within 5 h. In both the unbuffered system and the pH = 2.95 system, the decay of T_2 is faster with respect to the same systems at $T = 25^\circ\text{C}$, which implies that the condensation rate is higher at $T = 50^\circ\text{C}$. In the higher pH system with $\phi_T(0) = 0.20$, where the gel did not percolate, the decay of T_2 is equally fast in the initial 2 h for both temperatures. However, the final value of T_2 is much higher at $T = 50^\circ\text{C}$, which indicates that the relaxation behavior is similar to that of a normal liquid. Although the calibration gels were aged for 20 days, the final values of T_2 in the bulk experiments agree well with those of the calibration gels, and show a similar dependence of T_2 on pH and temperature.

It was found in a previous work that a minimum (plateau) in T_2 (for ^1H in H_2O in that case) corresponded with macroscopic

gelation of the aqueous phase as determined by tilting test tube experiments.⁴ In the tilting test tube experiments, the gel time is the time at which the sol–gel loses its ability to flow. The dimensions of the transparent test tubes (vials) were almost identical to the those of the Teflon vials used in the NMR experiments, so that the possible effect of container size¹⁵ on the gel time is minimized. Similar experiments were done in this work (at 35 °C) to confirm the relation between the gel transition and the minimum (plateau) in T_2 for ^2H . Again, a good agreement was found, and therefore the point at which the minimum or plateau in T_2 is found is used to derive the gel time. The results are listed in Table 3. The gel time varies between 0.5 and 30 h. The shortest gel times are found for the pH = 5.50 system followed by the unbuffered system and the pH = 9.48 system. The longest gel times are found for the pH = 2.95 system. Slow condensation rates are expected when the pH is close to 2.5, which corresponds to the isoelectric point of silica.^{1,6} Condensation is fast at neutral conditions,^{1,6} which explains why the pH = 5.50 system gelled faster than the other systems. The gel time decreases roughly by a factor of 2 when $\phi_{\text{T}}(0) = 0.35$ compared to the case when $\phi_{\text{T}}(0) = 0.20$. Increasing the temperature from 25 to 50 °C results in a reduction of the gel time of at least 50%. The effect of pH on the reaction rates was only determined for a limited set of buffers (chemicals). Preparing the buffers with other chemicals or concentrations is likely to quantitatively influence the results.⁶

5. Conclusion

The mechanisms of coupled mass transfer and gel reaction of TMOS in the two phase systems were revealed using a combined ^1H and ^2H NMR technique. The pH of the aqueous phase is the main parameter that affects the mass transfer and the gelation rates. The mass transfer of TMOS is driven by the rate of hydrolysis. Around pH = 6, the rate is minimum, whereas the hydrolysis rates, and thus the mass transfer rates, are increased in the acid- and base-catalyzed systems (because of the enhanced protonation of TMOS and the enhanced attack by hydroxyl anions, respectively). At a temperature of 50 °C, the rates are increased by a factor between 1.6 and 13 with respect to a temperature of 25 °C, depending on the pH used. The measurement of T_2 of deuterium in the calibration gels

showed that T_2 decreases with increasing initial TMOS content in the gelling solutions. The differences in T_2 for a given concentration among the various series, prepared with the different buffers, can be explained by the pH, which influences the microscopic structure of the silica gel. The gel transition times, derived from the T_2 versus time graphs, revealed that the gelation rates were the highest for the pH = 5.50 systems (gel time on the order of 1 h) and the lowest for the pH = 2.95 systems (gel time up to 30 h). Slow condensation rates are expected when the pH is close to 2.5, which corresponds to the isoelectric point of silica. Increasing the temperature from 25 to 50 °C results in a reduction of the gel time of at least 50%.

Acknowledgment. This research was supported by the Dutch Technology Foundation (STW) through project DAR 5756. Additional support was provided by Shell, INA Naftaplin, Chevron, Statoil, Conoco-Philips, and Gaz de France.

References and Notes

- (1) Brinker, C. J.; Scherer, G. W. *Sol-Gel Science: The Physics and Chemistry of Sol-Gel Processing*; Academic Press, Inc.: New York, 1990.
- (2) Plazanet, V.; Thomere, R. Institut National de la Propriété Industrielle Patent No. 2,624,198, Paris, 1989.
- (3) Zitha, P. L. J. *Well Treatment and Water Shutoff by Polymer Gels*; Delft University Press: Delft, The Netherlands, 2000.
- (4) Castelijns, H. J.; Huinink, H. P.; Pel, L.; Zitha, P. L. J. *J. Appl. Phys.* **2006**, *100*, 024916.
- (5) Castelijns, H. J.; Huinink, H. P.; Zitha, P. L. J. *Colloids Surf., A*, in press.
- (6) Brinker, C. J. *J. Non-Cryst. Solids* **1988**, *100*, 31–50.
- (7) Abragam, A. *The Principles of Nuclear Magnetism*; Oxford University Press: Oxford, 1961.
- (8) Woessner, D. E.; Zimmerman, J. R. *J. Phys. Chem.* **1963**, *67*, 1590–1600.
- (9) Benesi, A. J.; Grutzeck, M. W.; O'Hare, B.; Phair, J. W. *J. Phys. Chem. B* **2004**, *108*, 17783–17790.
- (10) Zimmerman, J. R.; Brittin, W. E. *J. Phys. Chem.* **1957**, *61*, 1328–1333.
- (11) Liu, G.; Li, G.; Jonas, J. *J. Chem. Phys.* **1991**, *95*, 6892–6901.
- (12) Yoshida, K.; Kitajo, A.; Yamaguchi, T. *J. Mol. Liquids* **2006**, *125*, 158–163.
- (13) Ludwig, R. *Chem. Phys.* **1995**, *195*, 329–337.
- (14) Lours, T.; Zarzycki, J.; Craievich, A. F.; Aegerter, M. A. *J. Non-Cryst. Solids* **1990**, *121*, 216–220.
- (15) Anglaret, E.; Hasmy, A.; Jullien, R. *Phys. Rev. Lett.* **1995**, *75*, 4059–4062.